IEEE TRANSACTIONS ON CONTROL SYSTEMS TECHNOLOGY - to appear

DOI 10.1109/TCST.2015.2493119

Control of Gear Transmission Servo Systems with Asymmetric Deadzone Nonlinearity

Zongyu Zuo, *Member, IEEE,* Xiaoliang Ju, and Zhengtao Ding, *Senior Member, IEEE*

***Abstract*—This brief deals with the output control problem of Gear Transmission Servo (GTS) systems with asymmetric deadzone nonlinearity between states. To overcome the difficulty of controller design due to the non-differentiability of the deadzone, a brand new differentiable asymmetric deadzone model is put forward, which provides an additional design degree of freedom to approximate the real deadzone with any prescribed accuracy. Based on the differentiability of the new model, a global differential homeomorphism and a simple state feedback controller are proposed to solve the output control problem. Finally, simulation studies are included to demonstrate the main results in this brief.**

***Index Terms*—Deadzone, differentiability, gear transmission servo systems, state feedback control.**

I. Introduction

BACKLASH (including deadzone, hysteresis) nonlinearity in the industrial motion control system frequently occur, which severely limits the dynamic performance and steady state precision of controlled systems. Deadzones, as one of the most important nonsmooth nonlinearities, exist ubiquitously in mechanical devices like gear transmission servo (GTS) systems. It is quite challenging to compensate the influence of deadzone nonlinearity because of the non-differentiable property of the conventional deadzone model. If the impact of backlash nonlinearity cannot be alleviated or eliminated, the induced limit cycle may exacerbate the stability of the controlled systems. In addition, the collisions between gears may produce serious concussion and noise. Since the 1940s, the study of the nonlinearity of nonsmooth deadzones has been of great interest among the high-precision mechanical control community.

In the past decades, many methods have been reported in literature, using adaptive control, variable structure control, intelligent control and nonlinear geometric theory etc., to tackle the backlash at the inputs/outputs or between states of controlled systems. No matter where the backlash locates, the nonlinearities like friction and saturation come with the controlled systems. The hysteresis model [1] is usually adopted for the backlash nonlinearity at the input or output, based on the assumption that the driven part of the controlled system keeps unchanged when the driving part is in the backlash period. The system with input/output hysteresis is usually transformed into a pseudo-linear system through inverse model compensation. With the aid of suboptimal convex optimization and Lyapunov tools, Tarbouriech et al. [2], [3] provided a constructive solution and the sufficient LMI conditions for the state feedback stabilization of systems with input backlash. Actually, the basic idea in [2], [3] also reveals that the systems with certain backlash nonlinearity can be characterized by general sector bounded nonlinear systems and the region of attraction for the closed-loop system can be identified by Lyapunov functionals with quadratic terms and generalized sector conditions via LMIs [4]. The results in [5] propose an analytic expression of backlash characteristic description with separated parameters using appropriate switching and internal functions. These papers deal with an exact model of backlash. In view of the systems in the presence of parameter uncertainties, neural network adaptive control [6], [7], fuzzy logic adaptive control [8], [9], and sliding mode control [10] have been employed in the control system design. The system with backlash nonlinearity between states, such as an electric mechanical actuator (EMA) system, can be described by two subsystems with backlash. In consideration that it is more realistic to take the moments of inertia of both entities into account, the deadzone model [1] for backlash description is widely used due to its high coincidence with the physical reality [11]. This deadzone model well describes the backlash nonlinearity due to the transmission torque between the driving and driven parts of controlled systems, which however greatly complicates the control design problem. Although the inverse model compensation can be applied to such systems as in [12], [13], it is impossible for the input of the deadzone model (i.e., the displacement difference between the two sides) to jump instantly due to the existence of inertia. Therefore, the inverse model compensation for deadzone model is not preferable in engineering practice. The results in [14] put forward a new smooth inverse model for the backlash and propose a corresponding robust adaptive output controller, but the inverse model requires the differential signal of the control input. An alternative is to establish a multi-model switching system [10], [16], [17], [18] which consists of several subsystems and the controllers designed separately for each of them. Su et al. [19] proposed a continuous dynamic model to describe a class of backlash-like hysteresis and its solution has a linear form with respect to the input signal, which facilitates controller design, such as the adaptive backstepping designs in [19], [20]. However, the parameter in this hysteresis model cannot be chosen

This work was supported by the National Natural Science Foundation of China (No.61203022), the Aeronautic Science Foundation of China (2012CZ51029), and the China Scholarship Council (CSC).

Z. Zuo is with the Seventh Research Division, Beihang University (aka Beijing University of Aeronautics and Astronautics, BUAA), Beijing 100191, China and an academic visitor at University of Manchester, Manchester M13 9PL, UK. e-mail: zzybobby@buaa.edu.cn.

X. Ju is with School of Automation Science and Electrical Engineering, Beihang University (BUAA), Beijing 100191, China.

Z. Ding is with School of Electrical and Electronic Engineering, University of Manchester, Manchester M13 9PL, UK.

freely due to the approximation requirement. In [15], Zou et al. transformed the hysteresis operator into an equivalent linear time-varying system with uncertainties, where the novel $\mathcal{L}_1$ adaptive controller can be applied. Similarly, taking into account of the unknown parameters in the deadzone model, adaptive control [16], [17], optimal predictive control [18] and sliding mode control [10] have been adopted in the existing literature to deal with the parametric uncertainties, which significantly complicates the control design of the systems with backlash nonlinearity between states.

It has been proved that limit cycles occur if the classical PD/PI-Load control are applied to such systems [1]. Motivated by the high precision control requirement in real-life engineering practice, this brief studies the output control problem of GTS systems in the presence of asymmetric deadzone nonlinearity. A new asymmetric differentiable deadzone model is developed, based on which the system dynamics are transformed into the perturbed state space model for controller design under a group of new coordinates. To elaborate the idea and the contribution, a simple state feedback controller is proposed as a benchmark for the output control problem of the mechanical systems with non-differentiable deadzone nonlinearity. The closed-loop stability and the tracking performance are established by using input-output stability theorem, from which one may find that the output tracking performance can be improved systematically by an extra degree of freedom in design provided by the new deadzone model. In addition, the employment of this new model in the controller design effectively eliminates the occurrence of limit cycles, which is validated via simulation. To the best of knowledge of the authors, it is the first time that an asymmetric differential deadzone approximation model is presented with arbitrary precision.

This brief is organized as follows: Section II presents the GTS system dynamics and a new asymmetric differentiable deadzone model. Section III proposes a global coordinate transformation and a state feedback controller. In section IV, an illustrative simulation example and a further performance comparison with a PD controller are discussed. Finally, the brief is ended by concluding remarks in section V.

Notation: The notations we use in this brief are fairly standard. $\|\cdot\|$ and $\|\cdot\|_\infty$ stand respectively for the Euclidean norm and the infinity norm, and $\mathbb{I}$ for the identity matrix with a proper dimension. However, with a slight abuse of notation, this brief interchangeably uses time-domain and frequency-domain language for representation of signals. For example, $\xi(t)$ and $\xi(s)$ denote the function of time and its Laplace transform, respectively. In the interest of brevity we omit arguments of a function without ambiguity after defining them.

II. Problem Statement

This section investigates the GTS system dynamics with asymmetric deadzone nonlinearity, and introduces a brand new asymmetric differentiable deadzone model to overcome the non-differential 'hard' property of the conventional deadzone, which greatly facilitates the controller in practice.

A. Dynamic Model of GTS Systems

A general dynamical model of GTS systems can be derived as follows [1]

$$\begin{cases} J_m \frac{\mathrm{d}^2\theta_m}{\mathrm{d}t^2} + c_m \frac{\mathrm{d}\theta_m}{\mathrm{d}t} = \tau - \mathrm{Dead}[\theta], \\ J_l \frac{\mathrm{d}^2\theta_l}{\mathrm{d}t^2} + c_l \frac{\mathrm{d}\theta_l}{\mathrm{d}t} = N_0 \mathrm{Dead}[\theta], \end{cases} \tag{1}$$

where J_m, θ_m and c_m are the moment of inertia, position and viscous friction coefficient of the driving side, respectively, J_l, θ_l and c_l the moment of inertia, position and viscous friction coefficient of the load side, respectively, N_0 the reduction ratio, τ the control input (torque), $\theta = \theta_m - N_0\theta_l$ the relative displacement, $\mathrm{Dead}[\theta]$ the transmission torque, defined by

$$\mathrm{Dead}[\theta] = \begin{cases} k_r(\theta - \alpha_r), & \text{if } \theta \geq \alpha_r, \\ 0, & \text{if } -\alpha_l < \theta < \alpha_r, \\ k_l(\theta + \alpha_l), & \text{if } \theta \leq -\alpha_l, \end{cases} \tag{2}$$

where $k_l \in \mathbb{R}^+$ and $k_r \in \mathbb{R}^+$ denote the rigidity coefficients, $\alpha_l \in \mathbb{R}^+$ and $\alpha_r \in \mathbb{R}^+$ the break points.

Remark 1: The deadzone model (2) well describes the transmission torque between the driving and driven parts of controlled systems. It is widely used for its high coincidence with the physical reality. In addition, the deadzone description (2) is a typical and important non-differentiable nonlinear factor in control theory research. In the real-life engineering practice, the parameters of transmission gears (i.e., k_l, k_r, α_l, α_r and N_0) may be obtained from the product specification.

B. Differentiable Asymmetric Deadzone Model

Some existing methods dealing with the 'hard' property use strong controls, which push the controlled systems to pass through the deadzone quickly. However, a collision at the deadzone end cannot be avoided. Motivated by this consideration, a new smooth asymmetric deadzone model is proposed as

$$T_s[\theta] = \frac{1}{\varrho} \ln \frac{1 + e^{\varrho k_r(\theta - \alpha_r)}}{1 + e^{-\varrho k_l(\theta + \alpha_l)}}, \tag{3}$$

where α_l, α_r, k_l and k_r are defined in (2), and ϱ is a positive adjustable parameter, called *soft degree* as will be clear in the following theorem.

Theorem 1: Consider the deadzone model (2) and the differentiable deadzone model (3). For any given deadzone parameters α_l, α_r, k_l and k_r, the approximation error, defined by $\eta(\theta) = \mathrm{Dead}[\theta] - T_s[\theta]$, can be made arbitrarily small if the parameter ϱ is sufficiently large, i.e., $\lim_{\varrho \to +\infty} |\eta(\theta)| = 0$.

Proof: First, it can be shown that $T_s[\theta]$ in (3) is monotonically increasing with respect to θ, since we have

$$\frac{\mathrm{d}T_s}{\mathrm{d}\theta} = \frac{k_r e^{\varrho k_r(\theta - \alpha_r)}}{1 + e^{\varrho k_r(\theta - \alpha_r)}} + \frac{k_l e^{-\varrho k_l(\theta + \alpha_l)}}{1 + e^{-\varrho k_l(\theta - \alpha_l)}} \geq 0,$$

where the equality holds if and only if $k_l = k_r = 0$. It follows that

$$\begin{cases} \frac{1}{\varrho} \ln \frac{2}{1 + e^{-\varrho k_l(\alpha_l + \alpha_r)}} = T_s[\alpha_r] \leq T_s[\theta] \\ \qquad < T_s[+\infty] = k_r(\theta - \alpha_r), & \text{if } \theta \geq \alpha_r, \\ -\frac{1}{\varrho} \ln \frac{2}{1 + e^{-\varrho k_l(\alpha_l + \alpha_r)}} = T_s[-\alpha_l] \leq T_s[\theta] \\ \qquad \leq T_s[\alpha_r] = \frac{1}{\varrho} \ln \frac{2}{1 + e^{-\varrho k_r(\alpha_l + \alpha_r)}}, & \text{if } -\alpha_l < \theta < \alpha_r, \\ k_l(\theta + \alpha_l) = T_s[-\infty] < T_s[\theta] \\ \qquad \leq T_s[-\alpha_l] = -\frac{1}{\varrho} \ln \frac{2}{1 + e^{-\varrho k_r(\alpha_l + \alpha_r)}}, & \text{if } \theta \leq -\alpha_l. \end{cases} \tag{4}$$

Next, for the conventional model $\mathrm{Dead}[\theta]$ in (2), it can be verified that

$$\frac{\mathrm{dDead}[\theta]}{\mathrm{d}\theta}=\begin{cases}k_r, & \text{if } \theta\geq\alpha_r,\\ 0, & \text{if } -\alpha_l<\theta<\alpha_r,\\ k_l, & \text{if } \theta\leq-\alpha_l,\end{cases} \tag{5}$$

which implies that $\mathrm{Dead}[\theta]$ is non-decreasing and monotonically increasing on $(-\infty,-\alpha_l]$ and $[\alpha_r,+\infty)$, respectively.

Using (2) and (3), we can write the approximation error $\eta(\theta)$ as

$$\begin{aligned}\eta(\theta)&\triangleq\mathrm{Dead}[\theta]-T_s[\theta]\\&=\begin{cases}k_r(\theta-\alpha_r)-T_s[\theta], & \text{if } \theta\geq\alpha_r,\\ -T_s[\theta], & \text{if } -\alpha_l<\theta<\alpha_r,\\ k_l(\theta+\alpha_l)-T_s[\theta], & \text{if } \theta\leq-\alpha_l.\end{cases}\end{aligned} \tag{6}$$

It follows from (4) and (5) that

$$\begin{cases}0=\eta(+\infty)<\eta(\theta)\\ \qquad\leq\eta(\alpha_r)=\frac{1}{\varrho}\ln\frac{1+e^{-\varrho k_r(\alpha_l+\alpha_r)}}{2}, & \text{if } \theta\geq\alpha_r,\\ -\frac{1}{\varrho}\ln\frac{1+e^{-\varrho k_l(\alpha_l+\alpha_r)}}{2}=\eta(-\alpha_l)<\eta(\theta)\\ \qquad<\eta(\alpha_r)=\frac{1}{\varrho}\ln\frac{1+e^{-\varrho k_r(\alpha_l+\alpha_r)}}{2}, & \text{if } -\alpha_l<\theta<\alpha_r,\\ -\frac{1}{\varrho}\ln\frac{1+e^{-\varrho k_l(\alpha_l+\alpha_r)}}{2}=\eta(-\alpha_l)\leq\eta(\theta)\\ \qquad<\eta(-\infty)=0, & \text{if } \theta\leq-\alpha_l,\end{cases} \tag{7}$$

which implies that

$$\begin{aligned}-\frac{1}{\varrho}\ln\frac{1+e^{-\varrho k_l(\alpha_l+\alpha_r)}}{2}&\leq\eta(\theta)\\ &\leq\frac{1}{\varrho}\ln\frac{1+e^{-\varrho k_r(\alpha_l+\alpha_r)}}{2}.\end{aligned} \tag{8}$$

Thus, $\lim_{\varrho\to+\infty}|\eta(\theta)|=0$ follows immediately, which completes the proof. ■

Remark 2: Theorem 1 demonstrates that the 'hard' property of the deadzone nonlinearity can be softened to any arbitrary precision by the new differentiable asymmetric deadzone model (3), as illustrated in Fig.1. Thus, ϱ in (3) is referred to as 'soft degree' of the controlled systems (1), and $\eta(\theta)$ as the softening error.

It is worthwhile mentioning that another new differential deadzone model [23] has been put forward when $k_l=k_r=k$, defined as

$$T_s'[\theta]=k\left(\theta+\frac{\alpha_l-\alpha_r}{2}\right)+\frac{k}{2\varrho}\ln\frac{\cosh(\varrho(\theta-\alpha_r))}{\cosh(\varrho(\theta+\alpha_l))}. \tag{9}$$

Further, if $\alpha_l=\alpha_r=\alpha$, then (9) degenerates into the differentiable symmetric deadzone model obtained in [24] as

$$T_s'[\theta]=k\theta+\frac{k}{2\varrho}\ln\frac{\cosh(\varrho(\theta-\alpha))}{\cosh(\varrho(\theta+\alpha))}. \tag{10}$$

Likewise, the deadzone approximation error with respect to the soften degree ϱ has been investigated in the existing literature, which is summarized in the following theorem.

Theorem 2: Consider the deadzone model (2) and the differentiable deadzone model (9) or (10). The approximation error, defined by $\eta(\theta)=\mathrm{Dead}[\theta]-T_s'[\theta]$, satisfies $|\eta(\theta)|<\frac{k\ln 2}{\varrho}$ and $\lim_{\varrho\to+\infty}|\eta(\theta)|=0$.

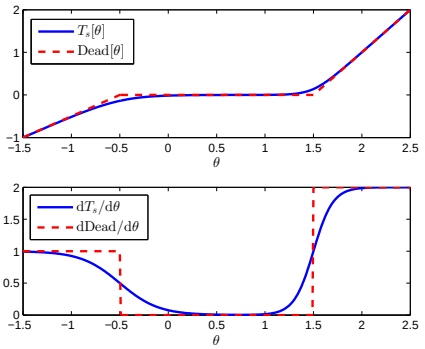

(a) $\varrho=5$

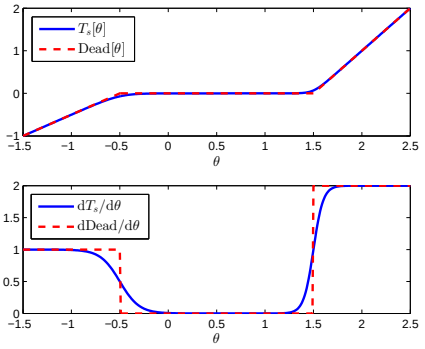

(b) $\varrho=10$

Fig. 1. Deadzone Approximation with Different Soft Degrees: $k_l=1;k_r=2;\alpha_l=0.5;\alpha_r=1.5$.

A natural question is whether the model derived in (9) or (10) is a special case of the model (3). The answer is negative, which is clarified in the following theorem.

Theorem 3: For $k_l=k_r=k$, the differential deadzone models (3) and (9) are equivalent if and only if $k=2$.

Proof: Let $\varphi_1=\theta-\alpha_r$ and $\varphi_2=-(\theta+\alpha_l)$ for notation simplicity. The gap between (3) and (9) can be written as

$$\begin{aligned}T_s-T_s'=&\frac{1}{\varrho}\ln\frac{1+e^{\varrho k(\theta-\alpha_r)}}{1+e^{-\varrho k(\theta+\alpha_l)}}-k\left(\theta+\frac{\alpha_l-\alpha_r}{2}\right)\\&-\frac{k}{2\varrho}\ln\frac{\cosh(\varrho(\theta-\alpha_r))}{\cosh(\varrho(\theta+\alpha_l))}\\=&\frac{1}{\varrho}\ln\frac{1+e^{\varrho k(\theta-\alpha_r)}}{1+e^{-\varrho k(\theta+\alpha_l)}}-\frac{1}{\varrho}\ln\left[\frac{1+e^{2\varrho(\theta-\alpha_r)}}{1+e^{-2\varrho(\theta+\alpha_l)}}\right]^{\frac{k}{2}}\\=&\frac{1}{\varrho}\ln\frac{1+e^{\varrho k\varphi_1}}{(1+e^{2\varrho\varphi_1})^{\frac{k}{2}}}-\frac{1}{\varrho}\ln\frac{1+e^{\varrho k\varphi_2}}{(1+e^{2\varrho\varphi_2})^{\frac{k}{2}}},\end{aligned} \tag{11}$$

from which it follows that $T_s-T_s'=0$ if and only if $k=2$. This completes the proof. ■

For the case $k\neq 2$, a further quantitative comparison between (3) and (9) may be made. Since the both functions (3) and (9) are odd symmetric with respect to the point $C(\frac{\alpha_r-\alpha_l}{2},0)$, without loss of generality we focus only on the gap between (3) and (9) for $\frac{\alpha_r-\alpha_l}{2}\leq\theta\leq\alpha_r$. It follows from (2), (3), (7) and (9) that $T_s[\theta]>\mathrm{Dead}[\theta]$ and $T_s'[\theta]>\mathrm{Dead}[\theta]$ for $\theta>\frac{\alpha_r-\alpha_l}{2}$, and $T_s[\theta]=T_s'[\theta]=\mathrm{Dead}[\theta]=0$ for $\theta=\frac{\alpha_r-\alpha_l}{2}$.

To facilitate the analysis, we define the following auxiliary function

$$D(x) = \frac{1}{\varrho} \ln \frac{1 + e^{\varrho k x}}{(1 + e^{2\varrho x})^{\frac{k}{2}}}. \tag{12}$$

Differentiating $D(x)$ in (12) against x yields

$$\frac{\mathrm{d}D(x)}{\mathrm{d}x} = \frac{k(e^{\varrho k x} - e^{2\varrho x})}{(1 + e^{\varrho k x})(1 + e^{2\varrho x})},$$

which implies that

$$\frac{\mathrm{d}D(x)}{\mathrm{d}x} \begin{cases} > 0, & \text{if } k > 2, \\ < 0, & \text{if } 0 < k < 2. \end{cases} \tag{13}$$

Since $\theta > \frac{\alpha_r - \alpha_l}{2}$ is considered, we have $\varphi_1 > -\frac{\alpha_r + \alpha_l}{2}$ and $\varphi_2 < -\frac{\alpha_r + \alpha_l}{2}$, and thus $\varphi_1 > \varphi_2$ follows. Based on the piecewise monotonicity derived in (13), it is straightforward to obtain from (11) that

$$T_s - T_s' = D(\varphi_1) - D(\varphi_2) \begin{cases} > 0, & \text{if } k > 2, \\ < 0, & \text{if } 0 < k < 2. \end{cases}$$

Thus, the model (9) has a better approximation to (2) between the break points for $k > 2$ while the model (3) better for $0 < k < 2$.

Remark 3: The deadzone model derived in (3) is differentiable and approximates the conventional deadzone (2) with arbitrary precision. Different from the existing deadzone models in literature, the key feature of this brand-new model is more general, as it includes totally symmetric case. In addition, from the practical point of view, the backlash parameters may vary due to the concussion, abrasion and wear of the mechanical parts, which may destroy the original symmetry. Thus, the proposed asymmetric model is more practical in some occasions.

C. State Space Description of GTS Systems

Let $x = [x_1, x_2, x_3, x_4]^T = [\theta_l, \omega_l, \theta_m, \omega_m]^T \in \mathbb{R}^4$ be the state vector of a GTS system, where ω_l and ω_m denote the speed of the load side and driving side, respectively. It follows from (3) and (6) that the state space equations of the GTS system in (1) can be formulated as follows:

$$\begin{aligned} \begin{bmatrix} \dot{x}_1 \\ \dot{x}_2 \\ \dot{x}_3 \\ \dot{x}_4 \end{bmatrix} &= \begin{bmatrix} x_2 \\ \frac{N_0 T_s[x_\theta]}{J_l} - \frac{c_l}{J_l} x_2 + \frac{N_0 \eta(x_\theta)}{J_l} \\ x_4 \\ -\frac{T_s[x_\theta]}{J_m} - \frac{c_m}{J_m} x_4 - \frac{\eta(x_\theta)}{J_m} \end{bmatrix} + \begin{bmatrix} 0 \\ 0 \\ 0 \\ \frac{1}{J_m} \end{bmatrix} \tau, \\ y &= \begin{bmatrix} 1 & 0 & 0 & 0 \end{bmatrix} x = x_1, \end{aligned} \tag{14}$$

where $x_\theta \triangleq x_3 - N_0 x_1$.

The *control objective* is to design a full-state feedback controller with an appropriate selection of ϱ such that 1) the closed-loop system are stable for any given bounded reference signal $r(t)$ and 2) the output $y(t)$ tracks the step reference $r(t) = r^* = \text{const}$ with desired accuracy.

III. Controller Design

In this section, we first introduce a global coordinate transformation for controller design, and then a simple controller is proposed for output control problem of the GTS systems.

Since the relative degree of the system in (14) is 4, define a global differential homomorphism as

$$z = \begin{bmatrix} z_1 \\ z_2 \\ z_3 \\ z_4 \end{bmatrix} = \begin{bmatrix} x_1 \\ x_2 \\ \frac{N_0 T_s - c_l x_2}{J_l} \\ \frac{N_0 \iota(x_\theta)(x_4 - N_0 x_2)}{J_l} - \frac{c_l (N_0 T_s - c_l x_2)}{J_l^2} \end{bmatrix}, \tag{15}$$

where

$$\iota(x_\theta) = \frac{k_r e^{\varrho k_r (x_\theta - \alpha_r)}}{1 + e^{\varrho k_r (x_\theta - \alpha_r)}} + \frac{k_l e^{-\varrho k_l (x_\theta + \alpha_l)}}{1 + e^{-\varrho k_l (x_\theta + \alpha_l)}}. \tag{16}$$

Note that $\iota(x_\theta)$ in (16) satisfies $\min\{k_l, k_r\} = k_m \le \iota(x_\theta) \le k_M = \max\{k_l, k_r\}$, i.e. $\iota(x_\theta)$ is lower bounded away from zero. It is straightforward to verify from (15) that $|\frac{\partial z}{\partial x}| = (\frac{N_0 \iota}{J_l})^2 > 0$ holds. Thus, the coordinate transformation (15) is global.

Let

$$\lambda(x_\theta) = \frac{\varrho k_r^2 e^{\varrho k_r (x_\theta - \alpha_r)}}{[1 + e^{\varrho k_r (x_\theta - \alpha_r)}]^2} - \frac{\varrho k_l^2 e^{-\varrho k_l (x_\theta + \alpha_l)}}{[1 + e^{-\varrho k_l (x_\theta + \alpha_l)}]^2}.$$

Choose the control torque τ as

$$\begin{aligned} \tau = \frac{J_m}{N_0 \iota} \Bigg[& u - N_0 \lambda (x_4 - N_0 x_2)^2 + \frac{N_0 \iota}{J_m} (T_s + c_m x_4) - \\ & \left(\frac{c_l^2}{J_l} - N_0^2 \iota \right) \frac{N_0 T_s - c_l x_2}{J_l} + c_l N_0 \iota (x_4 - N_0 x_2) \Bigg], \end{aligned} \tag{17}$$

where u will be designed later. With (15) and (17), the system in (14) can be transformed into the following form

$$\begin{cases} \dot{z} = Az + bu + \sigma(t), \\ y = c^{\mathrm{T}} z, \end{cases} \tag{18}$$

where

$$A = \begin{bmatrix} 0 & 1 & 0 & 0 \\ 0 & 0 & 1 & 0 \\ 0 & 0 & 0 & 1 \\ 0 & 0 & 0 & 0 \end{bmatrix}, \ b = \begin{bmatrix} 0 \\ 0 \\ 0 \\ 1 \end{bmatrix},$$

$$\sigma(t) = \begin{bmatrix} 0 \\ \frac{N_0 \eta}{J_l} \\ -c_l \frac{N_0 \eta}{J_l^2} \\ -\frac{N_0 \iota \eta}{J_l J_m} + \left(\frac{c_l^2}{J_l^2} - \frac{N_0 \iota}{J_l} \right) \frac{N_0 \eta}{J_l} \end{bmatrix}, \ c = \begin{bmatrix} 1 \\ 0 \\ 0 \\ 0 \end{bmatrix}.$$

With the introduction of the deadzone model (3), the system modeling error $\sigma(t)$ needs to be investigated.

Lemma 1: The modeling error $\sigma(t)$ in (18) is uniformly bounded by

$$\|\sigma(t)\| \le \frac{1}{\varrho} \sigma^*, \tag{19}$$

where

$$\begin{aligned} \sigma^* = & \frac{N_0}{J_l} \sqrt{1 + \frac{c_l^2}{J_l^2} + \left(\frac{k_M}{J_m} + \frac{N_0 k_M}{J_l} - \frac{c_l^2}{J_l} \right)^2} \\ & \cdot \ln \frac{1 + e^{-\varrho k_m (\alpha_l + \alpha_r)}}{2}, \end{aligned}$$

where $k_m = \min\{k_l, k_r\}$ and $k_M = \max\{k_l, k_r\}$. In addition,

$$\lim_{\varrho \to +\infty} \|\sigma(t)\| = 0. \tag{20}$$

Proof: It follows from the definition of $\sigma(t)$ and the fact $k_m \le \iota(x_\theta) \le k_M$ that

$$\begin{aligned}\|\sigma(t)\| &= \frac{N_0}{J_l}\sqrt{1 + \frac{c_l^2}{J_l^2} + \left(\frac{k_M}{J_m} + \frac{N_0 k_M}{J_l} - \frac{c_l^2}{J_l}\right)^2}\,|\eta(x_\theta)| \\ &\le \frac{1}{\varrho}\sigma^*,\end{aligned}$$

where Theorem 1 is applied to obtain the second inequality. It further implies $\lim_{\varrho \to +\infty} \|\sigma(t)\| = 0$. ∎

Before proceeding to the controller design, two definitions and a lemma need to be presented.

Definition 1: For a signal $\xi(t) = [\xi_1(t), \xi_2(t), \ldots, \xi_n(t)]^{\mathrm{T}} \in \mathbb{R}^n$ defined for all $t \ge 0$, the $\mathcal{L}_\infty$ norm is $\|\xi(t)\|_{\mathcal{L}_\infty} = \max_{i=1,2,\ldots,n}(\sup_{\tau \ge 0}|\xi_i(\tau)|)$.

Definition 2: The $\mathcal{L}_1$ gain of an asymptotically stable and proper single-input single-output (SISO) system is defined as $\|H(s)\|_{\mathcal{L}_1} = \int_0^\infty |h(t)|\mathrm{d}t$, where $h(t)$ is the impulse response of $H(s)$.

Lemma 2 ([22]): For an asymptotically stable proper SISO system $H(s)$, if the input $r(t) \in \mathbb{R}$ is bounded, then the output $x(t) \in \mathbb{R}^n$ is also bounded, and $\|x(t)\|_{\mathcal{L}_\infty} \le \|H(s)\|_{\mathcal{L}_1}\|r(t)\|_{\mathcal{L}_\infty}$.

The following theorem presents a simple controller for the GTS system in the presence of deadzone nonlinearity.

Theorem 4: Consider the GTS system in (1) with the control input defined in (17). If u in (17) is given by

$$u(t) = -k^{\mathrm{T}} z(t) + k_g r(t), \tag{21}$$

where $k = [k_1, k_2, k_3, k_4]^{\mathrm{T}} \in \mathbb{R}^4$ is the control gain vector such that $A_c = A - bk$ is Hurwitz, $r(t)$ the uniformly bounded reference signal, and $k_g = -1/(c^{\mathrm{T}} A_c b)$ the feedforward gain, the closed-loop system is stable and the transient response of the output satisfies

$$\begin{aligned}\|y(t)\|_{\mathcal{L}_\infty} \le& \|c^{\mathrm{T}}(s\mathbb{I} - A_c)b\|_{\mathcal{L}_1}\|k_g r(t)\|_{\mathcal{L}_\infty} \\ &+ \frac{1}{\varrho}\|c^{\mathrm{T}}(s\mathbb{I} - A_c)\|_{\mathcal{L}_1}\sigma^* + \rho_{in},\end{aligned} \tag{22}$$

where $\rho_{in} = \|sc^{\mathrm{T}}(s\mathbb{I} - A_c)^{-1}b\|_{\mathcal{L}_1} z_0$. In addition, if the reference signal input $r(t) = r^*$ is a constant, the steady state output, defined by $y_{ss} = \lim_{t \to \infty} y(t)$, depends on ϱ. Furthermore, as a limiting case of ϱ, the steady state output satisfies

$$\lim_{\varrho \to +\infty} y_{ss}(\varrho) = r^*. \tag{23}$$

Proof: With the global coordinate transformation (15) and the control torque defined by (17), the system dynamics (1) can be transformed into (18). Substituting (21) into (18) gives

$$\begin{cases} \dot{z}(t) = A_c z(t) + bk_g r(t) + \sigma(t), \\ y(t) = c^{\mathrm{T}} z(t), \end{cases}, \quad z(t_0) = z_0. \tag{24}$$

Taking Laplace transformation of both sides of (24) yields

$$z(s) = (s\mathbb{I} - A_c)^{-1}bk_g r(s) + (s\mathbb{I} - A_c)^{-1}\sigma(s) + (s\mathbb{I} - A_c)^{-1}z_0,$$

and

$$y(s) = y_r(s) + y_\sigma(s) + c^{\mathrm{T}}(s\mathbb{I} - A_c)^{-1}z_0,$$

where $y_r(s) = c^{\mathrm{T}}(s\mathbb{I} - A_c)^{-1}bk_g r(s)$ and $y_\sigma(s) = c^{\mathrm{T}}(s\mathbb{I} - A_c)^{-1}\sigma(s)$. Since the matrix A_c is Hurwitz, using Lemma 2, we have

$$\begin{aligned}\|z(s)\|_{\mathcal{L}_\infty} =& \|(s\mathbb{I} - A_c)^{-1}b\|_{\mathcal{L}_1}\|k_g r(s)\|_{\mathcal{L}_\infty} \\ &+ \|(s\mathbb{I} - A_c)^{-1}\|_{\mathcal{L}_1}\|\sigma(s)\|_{\mathcal{L}_\infty} + \|s(s\mathbb{I} - A_c)^{-1}\|_{\mathcal{L}_1} z_0.\end{aligned}$$

It follows from the uniform boundedness of $r(t)$ and $\sigma(t)$ that the closed-loop system is stable. Similarly, the output signal of the closed-loop system is bounded by

$$\begin{aligned}\|y(s)\|_{\mathcal{L}_\infty} \le& \|y_r(s)\|_{\mathcal{L}_\infty} + \|y_\sigma(s)\|_{\mathcal{L}_\infty} + \rho_{in} \\ =& \|c^{\mathrm{T}}(s\mathbb{I} - A_c)^{-1}b\|_{\mathcal{L}_1}\|k_g r(s)\|_{\mathcal{L}_\infty} \\ &+ \|c^{\mathrm{T}}(s\mathbb{I} - A_c)^{-1}\|_{\mathcal{L}_1}\|\sigma(s)\|_{\mathcal{L}_\infty} + \rho_{in},\end{aligned}$$

where $\rho_{in} = \|sc^{\mathrm{T}}(s\mathbb{I} - A_c)^{-1}b\|_{\mathcal{L}_1} z_0$, and Lemma 2 is used. Since $\|\cdot\|_\infty \le \|\cdot\|$ and the bound in (19) is uniform, the bound above yields

$$\begin{aligned}\|y(s)\|_{\mathcal{L}_\infty} \le& \|c^{\mathrm{T}}(s\mathbb{I} - A_c)^{-1}b\|_{\mathcal{L}_1}\|k_g r(s)\|_{\mathcal{L}_\infty} \\ &+ \|c^{\mathrm{T}}(s\mathbb{I} - A_c)^{-1}\|_{\mathcal{L}_1}\frac{\sigma^*}{\varrho} + \rho_{in}.\end{aligned}$$

Further, if $r(t) = r^* = \mathrm{const}$, the steady-state output can be derived, using $y_{ss} = \lim_{s \to 0} sy(s)$ by the final value theorem, as

$$\begin{aligned}y_{ss} =& y_{ssr} + y_{ss\sigma} + y_{\rho in} \\ =& \lim_{s \to 0} sc^{\mathrm{T}}(s\mathbb{I} - A_c)^{-1}bk_g\frac{r^*}{s} + \lim_{s \to 0} sc^{\mathrm{T}}(s\mathbb{I} - A_c)^{-1}\sigma(s) \\ &+ \lim_{s \to 0}[sc^{\mathrm{T}}(s\mathbb{I} - A_c)^{-1}z_0] \\ =& r^* + \lim_{s \to 0} sc^{\mathrm{T}}(s\mathbb{I} - A_c)^{-1}\sigma(s),\end{aligned}$$

which depends on ϱ due to $\sigma(s)$. In view of the uniform boundedness of $y_\sigma(s)$ and Theorem 1, steady-state output component $y_{ss\sigma}$ is also bounded and $\lim_{\varrho \to +\infty}|y_{ss\sigma}| = 0$, which implies that the result in (23) holds. ∎

Remark 4: The selection of the feedforward gain $k_g = -1/(c^{\mathrm{T}} A_c^{-1} b)$ in (21) achieves zero steady-state error with respect to the step reference signal if $\sigma(t) = 0$. It is worth noting that $k_g(s)$ is a feedforward prefilter which can be redesigned using standard linear system theory for different reference signals.

Remark 5: However, the modeling error due to the introduction of a new approximated deadzone cannot be eliminated because it is unmatched. Fortunately, the new deadzone model provides an extra degree of freedom ϱ to achieve arbitrarily high precision in design for tracking a step reference signal. In addition, we want to highlight that the differentiability of the new model (3) provides great flexibility for the coordinate transformation (like the one given in (15)) and the controller design.

Remark 6: It is worth emphasizing that a tradeoff between the veracity of steady response and the placidity of transient response has to be evaluated when selecting ϱ. Extreme large ϱ will recover the non-differential deadzone and leads to very aggressive closed-loop responses, which may degrade the closed-loop performance due to the limited closed-loop bandwidth.

TABLE I
GTS SYSTEM PARAMETERS

Notations	Values	Notations	Values
J_l	$0.5\,[\mathrm{kg}\cdot\mathrm{m}^2]$	J_m	$0.01\,[\mathrm{kg}\cdot\mathrm{m}^2]$
α_l	$0.002\,[\mathrm{rad}]$	α_r	$0.001\,[\mathrm{rad}]$
k_l	$0.2\,[\mathrm{Nm/rad}]$	k_r	$0.3\,[\mathrm{Nm/rad}]$
c_l	$0.12\,[\mathrm{Nm/rad}]$	c_m	$0.1\,[\mathrm{Nm/rad}]$
N_0	5		

IV. SIMULATION

To evaluate the effectiveness of the proposed controller, the parameters of a GTS system (1) with the deadzone nonlinearity (2) employed as in [21] are shown in Table I. The initial states $x_1 = 2[\mathrm{rad}]$, $x_2 = 0.5[\mathrm{rad/s}]$, $x_3 = 10[\mathrm{rad}]$ and $x_4 = 1[\mathrm{rad/s}]$ are set in the simulation. The soft degree in (3) is selected with different values as $\varrho_1 = 2$ and $\varrho_1 = 20$ for comparison, respectively. The controller gain in (21) is fixed as $k = [81, 108, 54, 12]^{\mathrm{T}}$, which corresponds to the desired closed-loop poles at -3 in the complex plane with the algebraic multiplicity 4.

Consider the step reference signal given by $r(t) = 2[\mathrm{rad}]$. Fig. 2 shows the responses of the output (i.e., the position of load side) for different soft degrees, from which we see that the tracking accuracy can be improved by larger ϱ at the cost of more aggressive transient behavior. The time history of the control input is plotted in Fig. 3, which shows that the control effort is proportional to the soft degree. The phase plot in Fig. 4 demonstrates that no limit cycle occurs due to the introduction of the new smooth deadzone model in (3) for the controller design. Clearly, the simulation result validates that the new deadzone model based controller achieves the control objective with sufficient tracking performance.

To highlight the contribution of this brief, we made a performance comparison with a proportional derivative (PD) controller, defined by

$$\tau(t) = k_d\dot{e}(t) + k_p e(t), \tag{25}$$

where $e(t) = r(t) - x_1(t)$, k_p and k_d stand, respectively, for the proportional and the derivative gain. In the simulation, $k_p = 0.5$ and $k_d = 0.05$ are fixed without re-tuning any other parameters including initial states. Figs. 5 and 6 show the step response and phase plot of the closed-loop system with PD controller, from which we see that the constant oscillation and the limit cycle occur in the steady phase. Thus, the tracking performance under the controller proposed in this brief is more appealing in practice.

Finally, we end this section with an additional simulation scenario by considering a periodic square-wave profile as the reference input. Without any re-tuning the control parameters, Figure 7 shows the satisfactory output tracking performance without any undesired vibration, although there is a little lag at each switching instant of desired tracking direction when the backlash mode occurs (i.e., $\mathrm{Dead}[\theta] = 0$, $-\alpha_l < \theta < \alpha_r$). Figure 8 shows the benign control input responses during the transition between the backlash gap back and forth. To make a comparison in this scenario, a load observer [1] (also known as the Brandenburg's observer [25]) is introduced into the PD controller (25) for the system (1)–(2):

$$\text{Brandenburg's observer: } \begin{cases} J_m\dot{\hat{\omega}}_m = -c_m\hat{\omega}_m - \hat{T}_{\mathrm{Dead}} + \tau \\ \hat{T}_{\mathrm{Dead}} = k_o(\hat{\omega}_m - \omega_m) \end{cases}$$

$$\text{Controller: } \tau(t) = k_d\dot{e}(t) + k_p e(t) + k_s\hat{T}_{\mathrm{Dead}}, \tag{26}$$

where $\hat{T}_{\mathrm{Dead}}$ denotes the estimated transmission torque, k_o is the observer gain and $0 < k_s < 1$ is the partial compensation gain to avoid that the motor would be entirely decoupled from the load. It has been pointed out in [1] that the load observer based PD Control overcomes the limitations of PID control (e.g., the limit cycle). With $k_o = 1$ and $k_s = 0.6$ and without re-tuning other design parameters, the output tracking trajectories under the controller (25) and (26) are shown in Fig. 9, which demonstrates that the PD controller with the load observer is superior to the pure PD controller. By a further comparison with Fig. 7, we find that the closed-loop system with our controller has faster and better transient responses, which demonstrates the benefit of the proposed controller based on the newly-developed differentiable deadzone model.

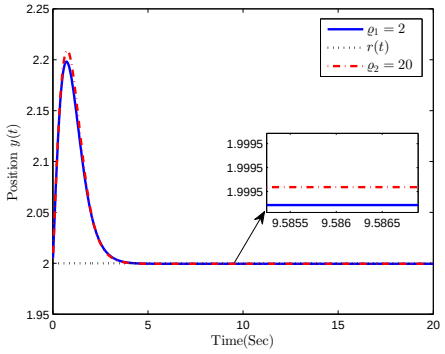

Fig. 2. System output: Step reference signal.

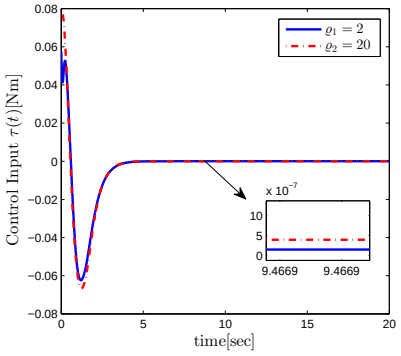

Fig. 3. Control torque: Step reference signal.

V. CONCLUSIONS

This brief presents a new asymmetric differentiable deadzone model for the controller design of GTS systems in the presence of asymmetric deadzone nonlinearity. A baseline state feedback controller is developed using this new model to

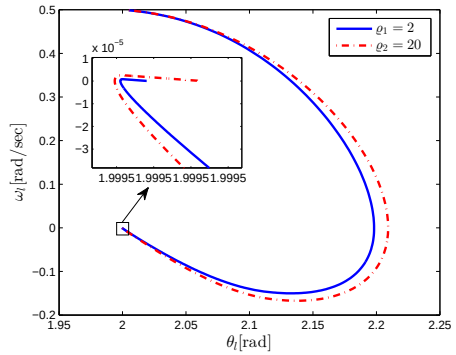

Fig. 4. Load phase portrait: Step reference signal.

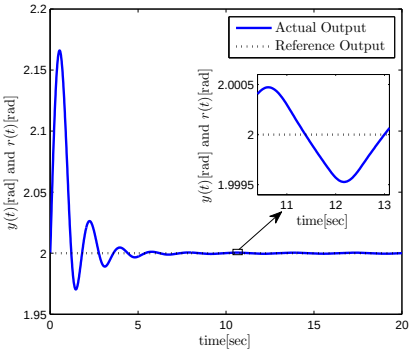

Fig. 5. System output: PD controller subject to step reference signal.

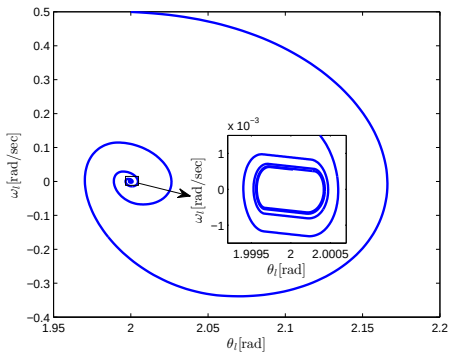

Fig. 6. Load phase portrait: PD controller subject to step reference signal.

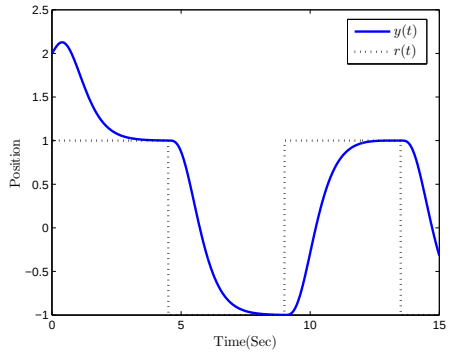

Fig. 7. System output: Square-wave reference input.

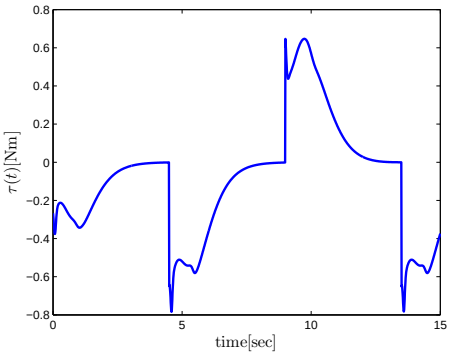

Fig. 8. Control torque: Square-wave reference signal.

achieve the output control, especially with assignable performance for the step reference signal. Future work includes the extensions to the output feedback control and adaptive control for parametric uncertainties in the deadzone model.

REFERENCES

[1] M. Nordin, and P.O. Gutman, "Controlling mechanical systems with backlash-a survey," *Automatica*, vol. 38, no. 10, pp. 1633–1649, Oct. 2002.

[2] S. Tarbouriech, C. Pieur, and I. Queinnec, "Stability analysis for lineaar systems with input backlash through sufficient LMI conditions," *Automatica*, vol. 46, no. 11, pp. 1911–1915, Nov. 2010.

[3] S. Tarbouriech, I. Queinnec, and C. Pieur, "Stability analysis and stabilization of systems with input backlash," *IEEE Trans. Autom. Control*, vol. 59, no. 2, pp. 488–494, Feb. 2014.

[4] B. Açikmeşe and M. Corless. "Stability analysis with quadratic Lyapunov functions: Some necessary and sufficient multiplier conditions." *Syst. Control Lett.*, vol. 57, no. 1, pp. 78-94, Jan. 2008.

[5] J. Vörös, "Modeling and identification of systems with backlash," *Automatica*, vol. 46, no. 2, pp. 369–374, Feb. 2010.

[6] J. Guo, B. Yao, Q.W. Chen, and X.B. Wu, "High performance adaptive robust control for nonlinear system with unknown input deadzone," in Proc. *IEEE CDC*, Dec. 2009, pp. 7675–7679.

[7] R.R. Selmic, and F.L Lewis, "Deadzone compensation in systems using neural motion control networks," *IEEE Trans. Autom. Control*, vol. 45, no. 4, pp. 602–613, Apr. 2000.

[8] R. Shahnazi, N. Pariz, and A.V. Kamyad, "Adaptive fuzzy output feedback control for a class of uncertain nonlinear systems with unknown deadzone-like hysteresis," *Commun. Nonlinear Sci. and Numerical Simulation*, vol. 15, no. 8, pp. 2206–2221, Aug. 2010.

[9] J.O. Jang, P.G. Lee, S.B. Park, and I.S. Ahn, "Deadzone compensation of systems using fuzzy logic," in Proc. *American Control Conference*, Jun. 2001, pp. 4788–4789.

[10] M.L. Corradini, A. Manni, and G. Parlangeli, "Variable structure control of nonlinear uncertain sandwich systems with nonsmooth nonlinearities," in Proc. *IEEE CDC*, Dec. 2007, pp. 2023–2028.

[11] G. Tao, and P.V. Kokotovic, "Adaptive control of plants with unkonwn dead-zones," *IEEE Trans. Autom. Control*, vol. 39, no. 1, pp. 59–68, Jan. 1994.

[12] N.J. Ahmad, H.K. Ebraheem, M.J. Alnaser, and J.M. Alostath, "Adaptive control of a DC motor with uncertain deadzone nonlinearity at the input," in Proc. *Chinese Control and Decision Conference*, May 2011, pp. 4295–4299.

[13] P. Yu, Z.B. Zhao, and G.J. Bao, "Inverse compensation method for the executor with deadzone based on adaptive inverse control," in Proc. *International Conference on Machine Learning and Cybernetics*, Aug. 2007, pp. 583–587.

[14] J. Zhou, C. Zhang, and C. Wen, "Robust adaptive output control of uncertain nonlinear plants with unknown backlash nonlinearity," *IEEE Trans. Autom. Control*, vol. 52, no. 3, pp. 503–509, Mar. 2007.

[15] X. Zou, J. Luo, and C. Cao, "Adaptive control for uncertain hysteresis

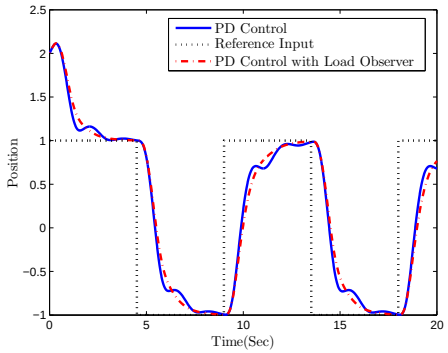

Fig. 9. System output: PD controller subject to square-wave reference signal.

systems," *ASME J. Dyn. Syst., Meas., Control*, vol. 136, no. 1, pp. 011011-1–011011-7, Jan. 2014.

[16] L.D.S. Coelho, and M.A.B. Cunha, "Adaptive cascade control of a hydraulic actuator with an adaptive dead-zone compensation and optimization based on evolutionary algorithms," *Expert Syst. with Appl.*, vol. 38, no. 10, pp. 12262–12269, Sep. 2011.

[17] M.B. Khan, F.M. Malik, and K. Munawar, "Switched hybrid speed control of elastic systems with deadzone," in Proc. *IEEE Int. Conf. on Industrial Engineering and Engineering Management*, Oct. 2010, pp. 1641–1644.

[18] P. Rostalski, T. Besselmann, M. Barić, F. Van Belzen, and M. Morari, "A hybrid approach to modelling, control and state estimation of mechanical systems with backlash," *Int. J. Control*, vol. 80, no. 11, pp. 1729–1740, Nov. 2007.

[19] C.Y. Su, Y. Stepanenko, J. Svoboda, and T.P. Leung, "Robust adaptive control of a class of nonlinear systems with unknown backlash-like hysteresis," *IEEE Trans. Autom. Control*, vol. 45, no. 12, pp. 2427–2432, Dec. 2000.

[20] J. Zhou, C. Wen, and Y. Zhang, "Adaptive backstepping control of a class of uncertain nonlinear systems with unknown backlash-like hysteresis," *IEEE Trans. Autom. Control*, vol. 49, no. 10, pp. 1751–1757, Oct. 2004.

[21] L. Márton, and B. Lantos, "Control of mechanical systems with Stribeck friction and backlash," *Syst. Control Lett.*, vol. 58, no. 2, pp. 141–147, Feb. 2009.

[22] H.K. Khalil, *Nonlinear systems* (3rd ed.). Upper Saddle River, NJ: Prentice Hall, 2005.

[23] Z. Zuo, and Z. Shi, "Backstepping control for a GTS system with unknown partially-nonsymmetric deadzone nonlinearity," *Proc. Inst. Mech. Eng. C: J. Mech. Eng. Sci.*, Submitted, 2015.

[24] Z. Shi, and Z. Zuo, "Backstepping control for gear transmission servo systems with backlash nonlinearity," *IEEE Trans. Autom. Sci. Eng.*, vol. 12, no. 2, pp. 752–757, Apr. 2014.

[25] G. Brandenburg, "Stability of a speed controlled elastic two-mass system with backlash and Coulomb friction and optimization by a load observer," In Symposium: *Modelling and Simulation for Control of Lumped and Distributed Parameter Systems*, Lille, New Brunswich, NJ: IMACS-IFACS, pp. 107–113.